MAGNET DESIGN AND CONTROL OF FIELD QUALITY FOR TPS BOOSTER AND STORAGE RINGS

J. C. Jan#, C. Y. Kuo, C. H. Chang, H. H. Chen, Y. L. Chu, Y. T. Yu, F. Y. Lin, M. H. Huang, C. S. Yang, I. C. Sheng, C. S. Hwang, G. H. Luo, C. T. Chen, NSRRC, Hsinchu 30076, Taiwan

Abstract

High quality magnets were designed, fabricated and installed in the Taiwan Photon Source (TPS). The lattice of the storage ring (SR) is based on a double-bend achromat (DBA) structure with an emittance 1.6 nm-rad and a small dispersion in the straight sections. A concentric booster ring (BR) is designed and constructed to share the same tunnel with the SR. The first synchrotron light from the TPS storage ring at 3 GeV was observed on Dec. 31, 2014. This accomplishment indicated that the precision of the profile and the field quality of the magnets as well as the alignment of the girders attained world class. The integral multipole components of the SR-quadrupole and SR-sextupole magnets conform to strict specifications. The maximum offset of the measured mechanical center in the magnets is better than ±0.01 mm after feet-shim. The offset of the magnetic center of the magnets is better than ±0.02 mm, as inspected with a rotating-coil method. The field quality of the BR-dipole and BR-quadrupole magnets were within design errors and proved in the beam commissioning. A study of relative permeability of the vacuum chamber was implemented during testing of the hardware of the booster ring. The magnetic field was distorted by the nonentity relative permeability of the vacuum pipes. This field distortion caused by the vacuum pipe is discussed in this paper.

INTRODUCTION

The Taiwan Photon Source (TPS) is a third-generation synchrotron light source, constructed at the National Synchrotron Radiation Research Center (NSRRC). To accommodate the constraints of the existing building, the magnets of the storage ring (SR) and the booster ring (BR) are constructed in the same tunnel, forming a concentric arrangement. The SR and the BR are composed of 48 SR-dipoles, 240 SR-quadrupoles, 168 SR-sextupoles, 54 BR-dipoles, 84 BR-quadrupoles and 24 BR-sextupole magnets. Buckley System Ltd. (New Zealand) was awarded the main contract to provide 641 magnets for the SR and the BR; Danfysik A/S (Denmark) constructed 255 magnets for transfer lines and corrector magnets. The preliminary magnetic design and engineering of the magnet system began in 2005 [1-3]; the TPS project was approved in 2007. A one-section prototype including 23 magnets was fabricated in 2011. The mass production of magnets was begun in 2012. In total, 641 magnets of the SR and BR were delivered by Oct. 2013. The hardware installation and integration of the accelerator including magnets, vacuum chambers, girders and diagnostic tools completed in mid-August, 2014. The system integration and improvement were completed on Dec. 12, 2014. The first synchrotron light at 3 GeV was observed with no correction applied on Dec. 31, 2014. The design, fabrication and correction of TPS magnets are presented in reports [2, 4-5].

#janjc@nsrrc.org.tw

MECHANICAL ERROR AND QUALITY OF THE MAGNETIC FIELD

The precise pole profile of a magnet is manufactured by either a Computer Numerical Control Machine (CNC) or a Wire Electrical Discharge Machine (WEDM). The SR-dipole and long SR-quadrupole magnets are machined with a CNC Machine because of the long yoke length; other magnets are machined by WEDM. Figures 1(a), (b), (c) and (d) display the sketches and labels of pole profile for SR-dipole, BR-dipole, SR-quadrupole and SR-sextupole magnets, respectively. The yoke length of SR-dipole, short SR-quadrupole, long SR-quadrupole, SR-sextupole, BR-dipole (BH/BD) and BR-quadrupole (pure) magnets are labelled as DL_1, *SQL*, *LQL*, *SL*, DL_2 and *BQL*, respectively. The bore diameter of the BR-quadrupole magnets is labelled as *BQd*.

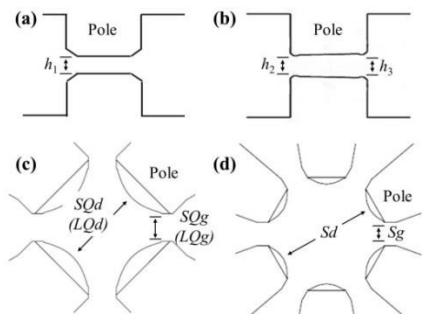

Figure 1: Pole profiles and labels of (a) SR-dipole, (b) BR-dipole, (c) short/long SR-quadrupole and (d) SR-sextupole magnets.

Table 1 lists the mechanical error (mean value±standard deviation) of the SR and BR magnets. The bore diameters of a long SR-quadrupole is counted without a yoke-shim [4]. The discrepancy between the designed and machined value of the bore diameter is better than 0.014 mm. The discrepancy between the designed and machined value of the pole gap of the SR magnet is better than 0.011 mm. The iron yokes of the SR and BR magnets are laminated with 1 and 0.5 mm of 50CS1300 silicon steel, respectively. The deviation of the laminated yoke length was controlled to be smaller than 0.15 % of the yoke length or one thickness of a lamination. The machining

errors of the bore diameter and yoke length of the BR-magnet are also listed at the Table 1. The machining dimensions of the diameter and yoke length of the BR magnets are close to the design values.

Table 1: Machining Quality of Various Magnets

Measure (Design) mean±sd, mm		Measure (Design) mean±sd, mm	
SR-dipole		BR-dipole (BD)	
h_1	45.484±0.07 (45.48)	h_2	21.400±0.009 (21.4)
DL_1	1026.23±0.46 (1026)	h_3	23.845±0.010 (23.84)
Short SR-quadrupole		DL_2	1553.89±0.21 (1554)
SQd	74.011±0.018 (74)	BR-dipole (BH)	
SQg	24.611±0.018 (24.6)	h_2	21.148±0.008 (21.14)
SQL	264.909±0.389 (265)	h_3	23.650±0.008 (23.64)
Long SR-quadrupole		DL_2	754.159±0.320 (754)
LQd	73.995±0.016 (74)	BR-quadrupole (pure)	
LQg	24.601±0.020 (24.6)	BQd	35.997±0.017 (36)
LQL	564.783±0.689 (565)	BQL	282.172±0.174 (282)
SR-sextupole			
Sd	(78)*		
Sg	18.298±0.020 (18.3)		
SL	226.997±0.315 (227)		

* No CMM data measured after pole-shim

Table 2: Field Quality of Various Magnets

	Measure @ 3GeV, mean±sd (Spec.)	
	SR-dipole	BR-dipole, BD/ BH
b_0L	-1.3201±0.0009	-1.3173±0.0019/ -0.6589±0.0007
b_1L	-	2.7719±0.0228/ 1.3922±0.0060
b_2L	-	9.9088±0.4514/ 4.3942±0.1146
	Short/Long SR-quadrupole	BR-quad., Q1
b_1L	-5.2160±0.0086/ -9.4438±0.0087	4.293±0.005
B_2L/B_1L	0.1±1.1/ 0.0±0.9(±2.0)	-1.4±3.0(±4.0)
B_3L/B_1L	-0.2±0.7/-1.7±1.0 (±2.0)	-4.3±1.6(±4.0)
B_5L/B_1L	-0.4±0.2/-0.3±0.3 (±0.8)	1.9±1.0(±3.0)
	SR-sextupole	
b_2L	120.216±0.306	
B_3L/B_2L	0.0±1.1(±2.0)	
B_4L/B_2L	0.3±1.3(±3.0)	
B_8L/B_2L	0.4±0.1(±0.5)	

Unit: b_0L (T·m), b_1L (T), b_2L (T/m), B_nL/B_mL ($\times 10^{-4}$)

Table 2 lists the main field dispersion and multipole errors of the SR and BR magnets [6]. The index of the dipole term is n=0 and of the quadrupole term is n=1. The dispersion of the field strength is generally dominated by the error of bore diameter and the yoke length. The multipole errors are dominated by asymmetry or machining error of the pole profile. The SR and BR magnets have excellent quality in the magnetic field because of the precisely controlled mechanical machining; the multipole errors of these magnets hence having much better performance than the specifications.

MAGNET CENTER SHIMMING AND INSPECTION

The precise center position of the magnets decreases the multipole errors of the dipole and quadrupole term for the quadrupole and sextupole magnet, respectively. The mechanical center, magnetic center, mechanical and magnetic tilt of the magnets were adjusted by using 3D-coordinate measuring machine (CMM) and then inspected with the rotating-coil measurement system (RCS) [6-7]. The mechanical-center offset of SR-quadrupole and SR-sextupole magnets were shimmed to better than ±0.01 mm using CMM after feet-shim [5]. The mean values of the magnetic center offset of the short SR-quadrupole (long SR-quadrupole) magnet is 0.003±0.009 (0.002±0.007) and 0.006±0.011 mm (0.007±0.009 mm) in vertical and horizontal direction, respectively. The mean value of the magnetic center offset of the SR-sextupole magnet is 0.005±0.008 and 0.005±0.009 mm in vertical and horizontal direction, respectively. The mean values of the mechanical and magnetic tilt of the SR-quadrupole and SR-sextupole magnets are better than 0.01° [6]. Figure 2 displays the measured closed orbit distortion (COD) without any corrector after LOCO and BBA [8]. The measured COD agrees with the simulation result that demonstrates very high quality of magnets and the girder alignments in the TPS [9].

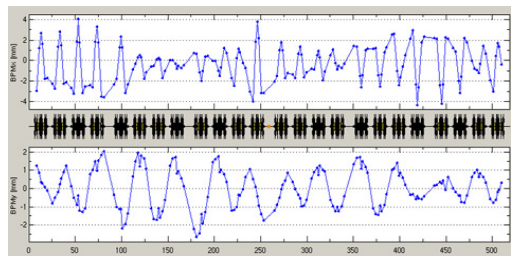

Figure 2: Measured COD without correctors in SR.

PERMEABILITY OF VACUUM CHAMBER

The vacuum pipes of the BR are composed of 181 elliptical and several circular cross-section chambers. These elliptical chambers are cold-drawn from circular tube of SUS304 stainless steel. The inner dimensions of the elliptical chamber are 35 mm (H) × 20 mm (V) and thickness 0.7 mm. After the drawing process, annealing was necessary to reduce the relative permeability of the chamber [10]. A NbFeB permanent magnet, corrector magnet and Hall-probe measurement system (HPS) were used for quick inspection of the permeability of the stainless steel vacuum pipes. A two-step test of the permeability of the vacuum chamber included a quick scan of the chamber using the NbFeB permanent magnet and the magnitude of permeability measured with the HPS. The chambers can be easily distinguished with this NbFeB magnet for $\mu_r > 1.002$. Figures 3(a) and (b) display the NbFeB magnet inspection before and after annealed chambers, respectively. The NbFeB magnet was

ISBN 978-3-95450-168-7

attracted by the chamber before annealing with high relative permeability. Figures 3(c) and (d) display the HPS to confirm the un-annealed chamber effect on field distortion. The ΔB_y is determined by the difference of B_y between the test chamber and without the chamber. The measurement stability at a fixed location of the HPS is better than 1×10^{-6} T for a short duration. A comparison between the TOSCA simulation and the HPS measurement of a chamber under a dipole field indicates the effects of various μ_r inducing B-field variation of a chamber. ΔB_y of 181 BR-chambers after annealing was less than $(2.0\pm1.1)\times10^{-6}$ T, which implies the μ_r of BR chamber to be approximately 1.002 after annealing.

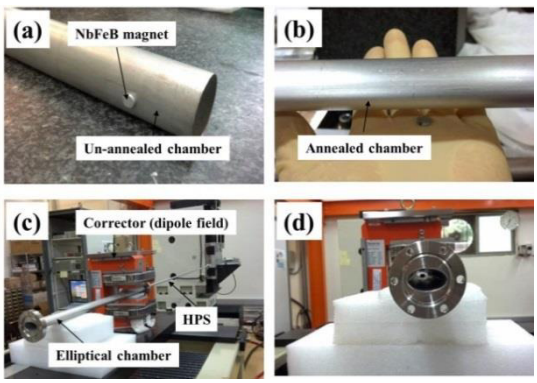

Figure 3: Inspect with NbFeB permanent magnet of (a) un-annealed chamber and (b) annealed chamber. Photographs (c) and (d) display the magnitude measurement of the μ_r using the HPS.

FIELD DISTORTION FROM THE UN-ANNEALED CHAMBER

An un-annealed chamber (μ_r~1.2) was used to understand the field distortion in the BR dipole (combined-function) magnet. The vertical field B_y in the BR-dipole magnet was measured by the HPS with scanning radius ±3 mm (*x*-*y* plane). The dipole field strength (b_0) and quadrupole field strength (b_1) of the BR-dipole magnet were analyzed from the B_y distribution.

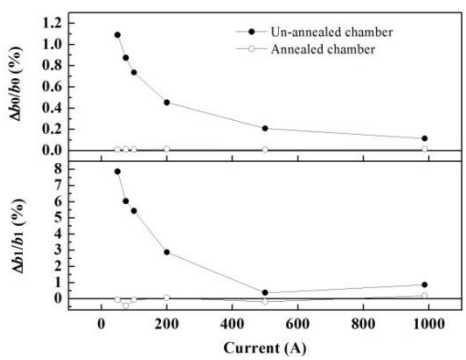

Figure 4: Field distortion vs. current variation of annealed and un-annealed chambers.

Figure 4 illustrates the *I*-*B* curve in $\Delta b_0/b_0$ and $\Delta b_1/b_1$ ratio of the annealed and before treatment chambers. The $\Delta b_0/b_0$ ($\Delta b_1/b_1$) is the distortion of dipole (quadrupole) field in the chamber. The field distortion increases as the excitation current decreasing in the untreated chamber. From the Fig. 4, it indicates that the orbit and behaviour of electron beam at low energy will be perturbed seriously due to the effect of un-annealed chamber in the BR.

SUMMARY

The machining errors of the pole profile of TPS magnet are better than ±0.02 mm as manufactured with CNC and WEDM techniques. The multipole errors of these magnets thereby conform to the strict requirements of the specifications. The deviation of the yoke length with iron-piece lamination was controlled to be less than 0.15 %. A precise mechanical and magnetic center was shimmed and corrected through CMM and RCS. The mechanical center offset was shimmed to better than ±0.01 mm in both vertical and horizontal directions. The magnetic center offset was determined to better than ±0.02 mm in both vertical and horizontal directions after CMM shimming. The mechanical and magnetic tilt of magnet is better than 0.01° after feet-shim. The relative permeability of the BR chamber is less than 1.002 after annealing treatment at 1050 °C in a vacuum furnace. All BR stainless-steel chambers were annealed to improve the field performance in booster.

REFERENCES

[1] C.H. Chang *et. al.,* "Conceptual design of magnet systems for the Taiwan photon source", in Proceedings of PAC, Knoxville, Tennessee, USA (2005).
[2] C. S. Hwang *et. al.,* "Status of accelerator lattice magnets design of TPS project", Proceedings of PAC 09, Canada (2009).
[3] F.Y. Lin *et. al.,* "Measurement of accelerator lattice magnet prototypes for TPS storage ring", Proceedings of IPAC, Kyoto, Japan (2010).
[4] J. C. Jan *et. al.,* "Design, construction, and performance of the TPS accelerator magnets", IEEE T. Appl. Supercon., V22, NO. 3, 4002304 (2012).
[5] J. C. Jan, *et. al.,* "Multipole errors and methods of correction for TPS lattice magnets", IEEE T. Appl. Supercon., V24, NO. 3, 4100905 (2014).
[6] J. C. Jan *et. al.,* "SUMMARY OF FIELD QUALITY OF TPS LATTICE MAGNETS", Proceedings of IPAC , Dresden, Germany (2014).
[7] J. C. Jan *et al.,* "Crosstalk issues between magnets in the synchrotron radiation accelerator", IEEE T. Appl. Supercon., V22, NO. 3, 9002004 (2012).
[8] C. C. Kuo *et. al.,* "Commissioning of the Taiwan Photon Source", TUXC3, this proceeding.
[9] T. C. Tseng *et. al.,* "The Auto-Alignment Girder System of TPS Storage Ring", THYB2, this proceeding.
[10] I. C. Sheng *et. al.,* "Demagnetized Booster Chambers in TPS", WEPHA049, this proceeding.